CHARACTERIZATION OF THE MICROSHELL SURFACE USING HOLOGRAPHIC MEASUREMENTS

F. SANDRAS,* C. HERMEREL, A. CHOUX, P. MÉRILLOT, G. PIN, and L. JEANNOT
Commissariat à l'Energie Atomique, Centre de Valduc, Département de Recherche sur les Matériaux Nucléaires Service Microcibles, 21120 Is Sur Tille, France

Received June 19, 2008
Accepted for Publication September 3, 2008

To characterize the shape, the quality, and the roughness of microshells, typically used technologies are scanning electron microscopy, scanning interferometric microscopy, or atomic force microscopy. One of the drawbacks of these techniques is that they are generally slow because of their scanning process. Digital holographic microscopy technology is an innovation that can offer ability adapted to these studies. It captures holograms instead of intensity images, as done by conventional microscopes. The holograms are then digitally interpreted (10 per second) to reconstruct a double image, one for the intensity and another one for the phase. Using a rotation axis, the bump counting for the complete microshell surface is possible with a very high speed. Using an image stitching software, mapping can be done in a few minutes. Wavelets such as "Mexican hat" are used to model the bumps. Each bump can then be characterized on the map by its position, diameter, and height.

KEYWORDS: *digital holography, surface defect mapping, wavelet analysis*

I. INTRODUCTION

The Laser Mégajoule (LMJ) project is the French project for inertial confinement.[1] The thermonuclear fusion shall be obtained by the implosion of a solid deuterium-tritium (D-T) fuel layer inside a CHGe spherical shell (Fig. 1). This amorphous hydrogenated carbon is the nominal ablator used to perform inertial confinement fusion (ICF) experiments. Coatings are prepared by glow discharge polymerization (GDP) with trans-2-butene and hydrogen and can be easily doped with germanium.

Laser fusion targets must have optimized characteristics: a 175-μm-thick spherical polymer shell with a 2.4-mm diameter, sphericity and thickness concentricity better than 99%, and an outer and an inner roughness of a few nanometers at high modes. In particular, careful attention must be paid to the surface roughness of the coating. In fact, the surface finish of these laser fusion targets must be extremely smooth in order to minimize hydrodynamic instabilities during experiments.

The GDP technique was found to be the most powerful process to improve the morphology, roughness, and homogeneity of deposits.[2,3] It is possible to obtain coatings without any growing structures and thus only with very small nodules at the surface by controlling the coating parameters and having low deposition rates. This allows one to obtain high mode roughness <10 nm. Nevertheless, this is not sufficient to obtain LMJ specifications especially at lower and intermediate modes that are strongly degraded by local defects, called "bumps" (illustrated in Fig. 2). They grow up during the coating in a cone shape from a single point.

Different studies have produced solutions to reduce microshell roughness, as the synthesis of graded germanium (Ge) microshells with helium adding in plasma, or with hydrogen pulses.[4] However, bumps still partially remain. Although the surface roughness is under the LMJ specifications without taking into account the bumps, microshell characteristics must also be in agreement with the isolated feature specification,[5] which defines the number and the allowed dimensions of large isolated surface defects over the entire capsule surface.

Up to now, roughness was characterized on some parts of the microshell surface with an interferometer and with a sphere mapper, based on atomic force microscopy (AFM) measurements. We need now to rapidly make a bump map of the entire microshell surface with the height and lateral size of each defect. Digital holographic microscopy (DHM) is a technique that gives information about the surface roughness of a sample at very high

*E-mail: florent.sandras@cea.fr

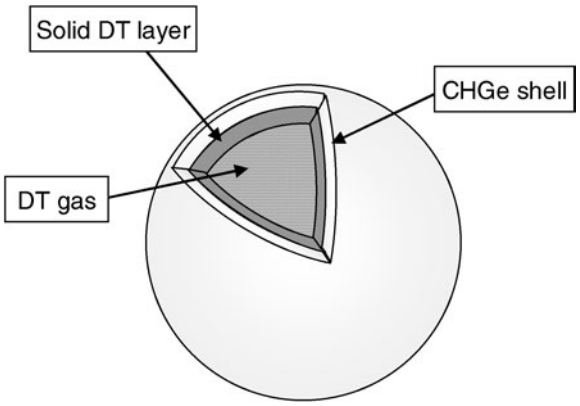

Fig. 1. Solid D-T layer in CHGe microshell.

rates and with a very good axial accuracy. Using a rotation axis, DHM enables characterizing roughness by acquisition of scans series along equators. The straightening out of the scan curvature and their stitching permit, with an appropriate number of equators, to map the entire microshell surface. At last, an analytic processing by wavelets gives positions, heights, and widths of all bumps existing on the microshell.

The content of the paper is as follows. First of all, the principle of the DHM will be reviewed and its use will be justified by comparison to other roughness characterization techniques. We will also present instrumental setup developed to cover the entire surface of a microshell.

In Sec. III, the processing of raw data will be described. Homemade software, developed under Labview™, makes a straightening out of images of the surface roughness by an automated shrinkage of the curvature radius, and a stitching using pattern matching is made on successive images to reconstruct the complete equators of the surface. Finally, a threshold level is applied to isolate the interfering higher defects present on each equator and to optimize the processing by wavelet transform in order to refine calculations of positions, heights, and lateral sizes of bumps on microshells.

Section IV will be devoted to the presentation of the final results compared to the isolated defect specifications to evaluate if their statistical distribution in number and dimension would affect the ignition attempt.

II. DHM, A POWERFUL TOOL FOR ROUGHNESS MEASUREMENTS

The study of roughness of the outer surface of the microshell is a sustained work[2–4,6,7] due to the importance of obtaining a surface as smooth as possible to optimize the ablator part played by the capsule in ICF experiments. Roughness has been characterized for some years by interferometry and using a sphere mapper.[3,7] The stringent specifications required for uniform Ge doped microshells have been demonstrated for modes higher than 100 with a very smooth background [root mean square (RMS) $<$ 10 nm] (Ref. 6) and recently with the reach of 10 nm in the middle range roughness (modes from 10 to 100) (Ref. 4). Nevertheless, persistent presence of local defects, called bumps (see Fig. 2), still deteriorates the global roughness. These bump diameters range from 40 to 60 μm and heights $<$1 μm. They grow up in a cone shape on a singular point. There have been numerous publications on the cause of these isolated domes: effect of the mandrel surface chemistry, presence of microscopic defects on the mandrel, abrasion damage from mechanical agitation, and deposition parameters. An isolated feature specification gives the number and size of bumps allowed on the entire microshell surface.

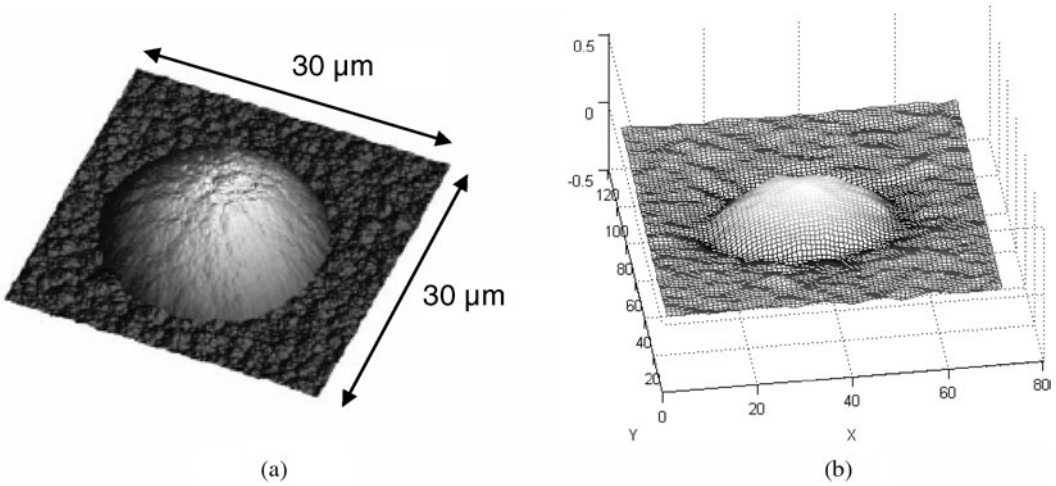

Fig. 2. Bump on microshell surface: (a) image with scanning electronic microscope and (b) 3-D plot with DHM acquisition.

DHM is the technique chosen to make in an automated way an entire mapping of the outer surface with high resolution and speed in agreement with our needs.

II.A. DHM Principle

Digital holographic microscopy is an imaging technique that enables quantitative measurement of both the amplitude and phase of the wave front reflected by a sample seen through a microscope objective. A hologram, composed by the interferences of the wave coming from the sample with a reference wave, is recorded with a camera. Then the hologram is numerically processed to extract both amplitude and phase information. Thanks to its interferometric nature, DHM provides phase images with a corresponding accuracy in the nanometer range along the optical axis of the objective, revealing extremely detailed information about the sample surface. The principle of DHM, from hologram acquisition to numerical reconstruction, is schematized in Fig. 3. Dynamic imaging in real time is practically achieved thanks to the actual performance of digital cameras and personal computers.

II.A.1. Classical and Digital Holography

Holography was invented in 1947 by Denis Gabor[8] and was really available at the beginning of the 1960s with the appearance of the first lasers, the only means of obtaining a sufficiently intense monochromatic light source. The principal idea of the technique is to record all the information contained in the backscattered light by an illuminated object. In fact, light is modified by the object in its two fundamental characteristics: its intensity, and phase. Variations in opacity affect the intensity, and differences in position change the phase because the light must travel different distances.

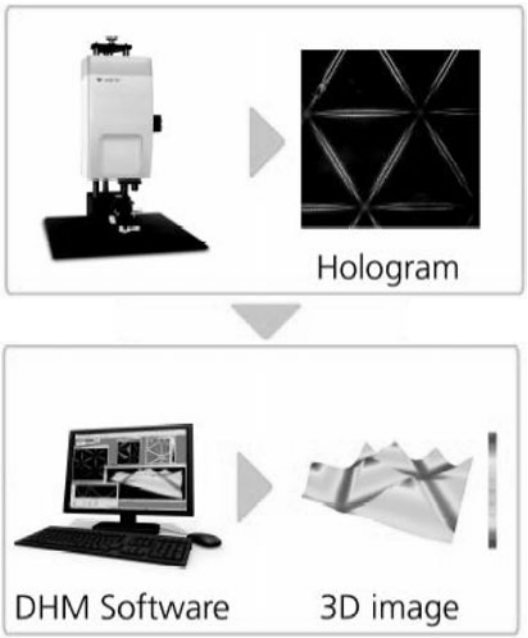

Fig. 3. Working principle of a DHM: capture of a hologram and numerical reconstruction of intensity and phase information using software for 3-D image.

A traditional image analysis is only sensitive to the intensity, and the variations of the phase are lost. Gabor demonstrated it was possible to keep the complete wave front on a photosensitive substrate in order to later read this hologram, reilluminating it with a reference wave. With a hologram, the observed objects can be represented as phase images, and quantitative three-dimensional (3-D) information is obtained.

In digital holography, the idea is to replace the recording of the hologram on the photosensitive substrate by an electronic camera, such as charge couple device (CCD) cameras or complementary oxide semiconductor cameras. Therefore, the cumbersome task of hologram developing is suppressed and high acquisition rates become available. CCD records the hologram, but the reconstruction is then done completely numerically.[9,10]

II.A.2. Experimental Configurations

The Swiss firm Lyncée Tec[11] supplied us with DHM and with the Koala™ software, which reconstructs and analyzes hologram data.

Figure 4 presents a digital holographic microscope scheme in reflection configuration: its basic architecture is derived from a modified Mach-Zehnder interferometer. The collimated source beam (laser diode) is separated in two: the object beam O and the reference beam R. The object beam illuminates the sample via the objective. The retro-diffused beam is collected by the objective of the microscope and recombined with R to form a hologram on the CCD camera.

A microshell, our sample, is maintained by aspiration with an adapted nozzle. This one is mounted on a rotation axis and allows scanning of the microshell along an entire equator. A second rotating nozzle is placed perpendicularly to the former. The combination of both permits characterization of the entire surface of the microshell. Motors performing rotations are driven by Koala™ software: it becomes possible to execute an automated scan along numerous equators in a very short lapse of time.

In order to characterize our microshell, we use a microscope objective with a numerical aperture of 0.5 defining $\times 20$ magnification. A windowing is applied on the CCD array to optimize acquisition and resolution. The region of interest (ROI) is limited to 650×650 pixels, which correspond to a 250×250 μm image. Such objective parameters and field of view give a lateral resolution <400 nm. This value was obtained with measurements on a standard. The axial resolution is defined

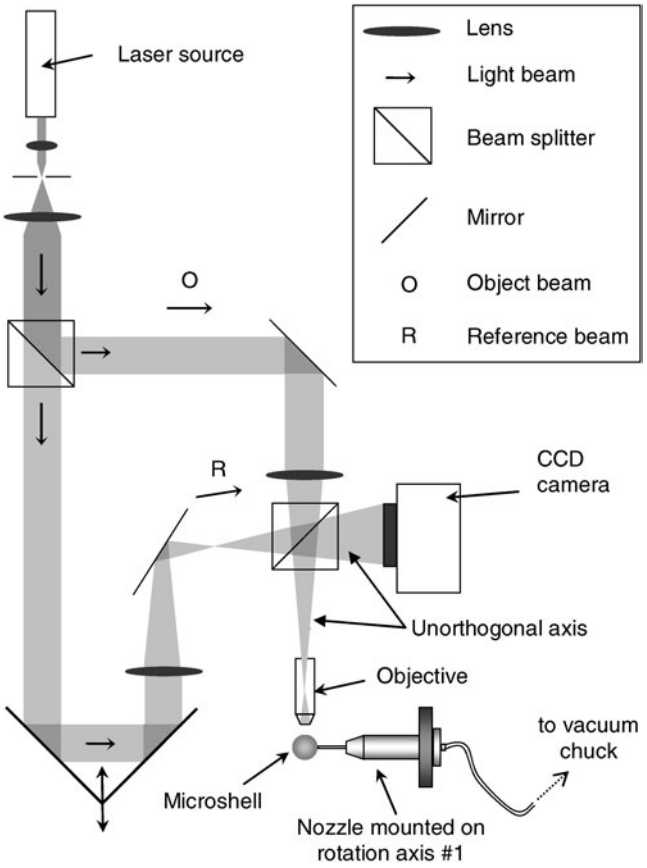

Fig. 4. Holographic microscope scheme in reflection scanning microshell surface. Microshell is maintained by aspiration. Two rotation axes, driven by computer, allow characterization of the entire surface of the microshell.

by the accuracy for phase measurements and depends on laser source wavelength (683 nm for our setup). For a homogeneous sample, the axial resolution reaches 0.1 nm. In hologram acquisition mode, the frame rate is 10 images per second; in reconstruction mode, it is 3 images per second. These "real time" conditions free us from vibrations that could disturb acquisition quality. Figure 5 presents a roughness image of the microshell surface from DHM acquisition.

II.B. Advantages of DHM in Bump Mapping over Interferometry and AFM

Digital holographic microscopy presents nanometric resolutions and an important acquisition rate, which give the possibility of making very impressive characterizations of the outer surface of a microshell. Up to now, roughness characterizations were only made with the interferometer and sphere mapper using AFM technology.

An optical interferometer using a white light enables observation and mapping of the microshell surface. Although it is more adapted to a plane sample, this technique can reach with some limitations to measurements of bump height (not roughness) on spherical samples. Very sensitive to object curvature, exploitable surfaces are limited by edge effects in 3-D plots during numerical reconstruction. Using an objective magnification ($\times 20$) with a $\times 0.5$ zoom, lateral resolution is ~ 900 nm with an image size of 450×450 μm. Axial resolution, depending on piezoelectric motor motions in the reference arm of the interferometer, is better than 1 nm. On the other hand, the technique is less desirable than DHM to get a map of the surface because of the necessary time delay to complete an acquisition (30 s per image). To analyze and count local defects on the entire surface of the microshell will require more than 1 day of acquisitions. DHM shows the same performances as interferometry with a higher acquisition rate: larger image size with the interferometer is no more an advantage and DHM minimizes the potential image deformation on edges.

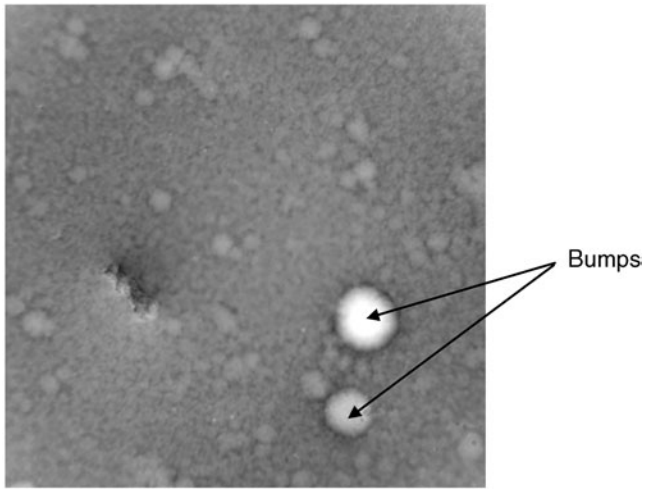

Fig. 5. DHM phase image (250×250 μm^2) of microshell surface.

The sphere mapper is an instrument dedicated to the measurement of surface roughness of microshells with high accuracy.[3] Surface profilometry is measured by an AFM tip that comes "in touch" (in fact very close) with the microshell held by aspiration. Detection of interatomic forces between the tip (associated with a cantilever with a fixed spring constant) and the sample surface creates tip moves. These shifts are quantified by a laser and are directly linked to height variations on the microshell surface. Axial resolution of the sphere mapper is <1 nm, and its lateral resolution is near 2 μm. Different modes of characterizations are possible: from a patch scan to a "full" sphere mapper. The former permits one to obtain images (to 100 μm $\times$ 100 μm) of the microshell surface with the move of the tip on the static sample: an accurate roughness measurement is possible on the image for the highest deformation modes. The second method consists of scanning the

surface along five principal profiles ("equators") of the microshell; each principal profile is composed of 16 secondary profiles, each spaced by 40 μm. So a principal profile corresponds to an equator with a 600-μm width. In this context, the entire surface of the microshell is scanned. This operation lasts around half a day.

The sphere mapper gives highly resolved data with a frame rate relatively well, but it is more sensitive to measurement noise due to vibrations. Moreover, it seems more adapted to measure background roughness of the microshell surface after shrinkage of local defects present on profiles. In fact, defects like bumps are observed but profile width (20 nm for the tip curvature radius) and space between each profile (40 μm) do not allow one to count precisely all defects and to give real bump sizes.

At last, contrary to both other techniques, DHM does not need the motion of mechanical parts. So, its wear is limited and no drifting is possible (the light source is used in reference); the interferometer and sphere mapper need some recalibration in time.

Thus, DHM appears to be the technique most adapted to make an entire mapping of the microshell surface (bump numbers, positions, and dimensions) with subnanometric axial resolution and very high acquisition rates.

III. PROCESSINGS OF DHM DATA

An important development schedule of softwares has been implemented to perform a quantitative analysis of data resulting from DHM acquisitions. The hologram reconstruction provides a phase plot of the scanned surface, which can be associated to 3-D topography. To get the entire map and to extract all information about bumps (positioning, height, and sizes), it is necessary to process raw data. First, a preprocessing is performed to reconstruct each equator in only one plane image, and then an analysis of data is made with a mathematical tool adapted to bump geometry: the analysis by wavelets.

III.A. Preprocessing of DHM Images

Phase images obtained with DHM present a curvature due mainly to the microshell. In order to characterize bumps correctly and measure their effective dimensions [height and full-width at half-maximum (FWHM)], these raw images must be straightened out with the calculation of the image curvature radius with the least mean squares method and the shrinkage of this baseline from phase data (or roughness data). Figure 6 shows a raw roughness image of a microshell obtained with DHM and the same with the processing of straightening out [3-D and two-dimensional (2-D) plots].

The entire mapping of a microshell is obtained doing roughness scans along numerous equators (with 12 equators, 95% of the surface is covered for a 2400-μm-diam microshell). For the production of an entire equator, successive roughness images are stitched by pattern-matching software. The rotation step between two DHM acquisitions is fixed to be lower than the angle corresponding to the covered surface on the microshell for one image. Thus, a region is common between two successive images, and errors due to the presence of bumps on the brink of images or due to approximation in rotation motions are minimized. Around 70 images are needed to reconstruct a full equator correctly.

Before applying analysis with wavelets on the bump map and in order to optimize it, each equator is subject to a threshold level. It allows extraction of ROIs from images, corresponding to local defect localization. The outcome is a significant saving of time in the following analysis, because it is just necessary to characterize large defects. Figure 7 presents the result of application of a 120-nm threshold level on an entire equator.

The result of this preprocessing is the localization of the largest bumps (large enough so that their presence could be disturbing on the microshell outer surface, according to bump curves) on numerous equators covering the entire surface of the microshell.

III.B. Wavelet Analysis on Data Issued from DHM Acquisitions

To obtain precisely the position and the dimensions of bumps present on the microshell surface, a wavelet analysis is used. The goal is to show the similarity between the DHM signal and characteristic waves. This correlation depends on different scale factors such as height, width, and position. Numerous wavelet scales will be tested on bump ROI to find the maximum correlation.

The form of wavelets used has been chosen after some specific studies to deal with the morphology of the usual local defects on the microshell surface. All imaging ways showed that defects are composed of a bump surrounded by a moat around its base. The wavelet form chosen for analysis is the one called "Mexican hat," illustrated in Fig. 8. Studies showed in particular that this type of wavelet is much more adapted to bump form in comparison to a wavelet with a Gaussian form (dome). Figure 9 presents the example of two bump profiles fitted with a Mexican hat wavelet and with a dome. In each case, FWHM of wavelets is calculated and compared to FWHM of bump. For different bump forms, the Mexican hat wavelet seems to be more adapted to model the defect with an appropriate FWHM in comparison with the one obtained with a Gaussian fitting.

The mathematical expression of the Mexican hat wavelet is

$$\Psi_{a,b}(x,y) = \frac{1}{a}\cdot\left(1-\frac{x^2+y^2}{a^2}\right) \cdot\exp\left[-\frac{(x-b)^2+(y-b)^2}{2a^2}\right], \quad (1)$$

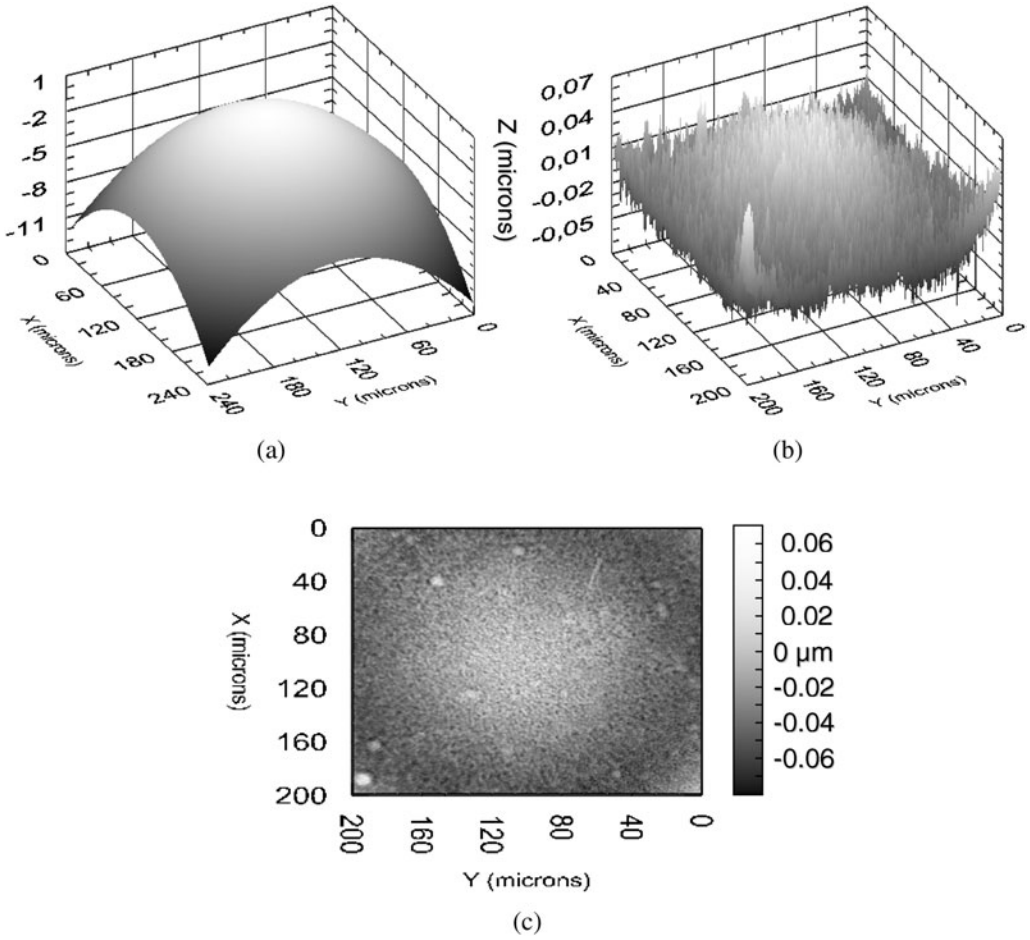

Fig. 6. DHM roughness image of a microshell: before processing (a) raw 3-D data, and after processing (b) straightened-out 3-D plot and (c) 2-D plot.

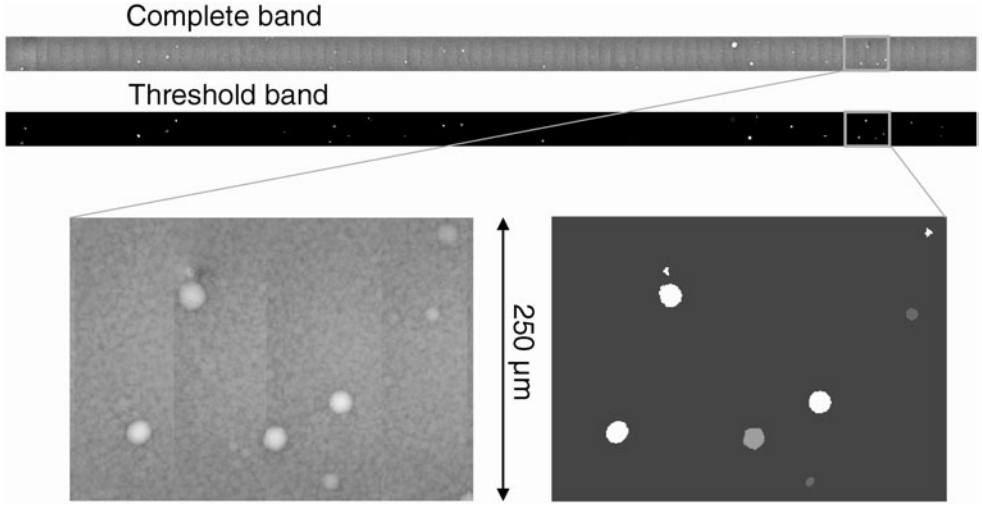

Fig. 7. Application of threshold level (120 nm) on a roughness data band corresponding to microshell equator.

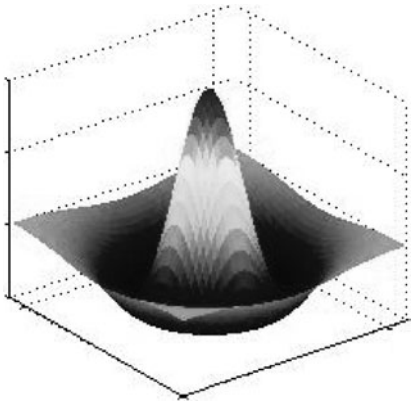

Fig. 8. Wavelets as "Mexican hat" are used to fit bump shape.

where

a = scale parameter

b = translation parameter corresponding to the signal position

x, y = surface coordinates.

For each bump, different wavelet scales are tested to find the maximum of correlation. For each test, a calculation in wavelet transform is made and a coefficient from a 2-D convolution is done. The maximum value of this coefficient is linked to a maximum correlation. The final result gives sizes (heights and FWHM) and positions for each bump selected with threshold level processing.

Some developments will be necessary to reduce redundancy in defect characterization for bumps that might occur in common regions at several bands.

IV. RESULTS OF BUMP CHARACTERIZATION

The entire processing of DHM acquisitions on the microshell gives localization and dimensions of all local defects present on the outer surface. The number and sizes of bumps are important parameters that justify microshell quality and validity for the ignition process. Theoretical studies[5] have set specifications about local defects over the entire outer surface of the microshell; the isolated feature specification defines the number and the allowed dimensions of the defects classed into three frequency regions. Figure 10 shows the graph illustrating this specification.

The DHM acquisitions followed by numerical treatment give height and size for each bump. Finally we can represent on a graph each defect and compare them to specification curves. If no defect is above the full line curve, less than 20 fit above the dashed curve, and less than 100 fit above the dotted curve, then the outer quality

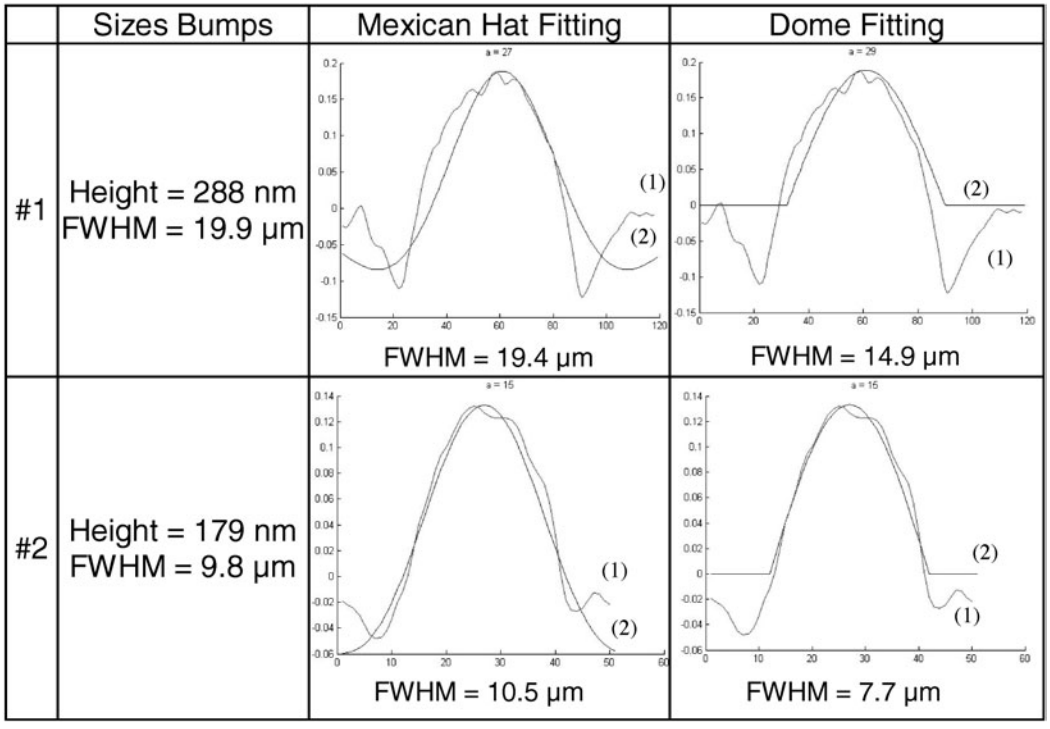

Fig. 9. Comparison of FWHM between (1) bumps and (2) two wavelet fittings. Scale unit is micrometers.

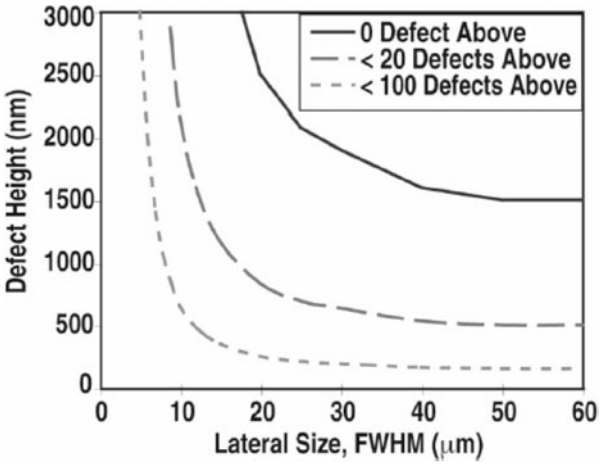

Fig. 10. The isolated feature specification defines the allowed number and dimensions of bumps on the outer surface of microshell.

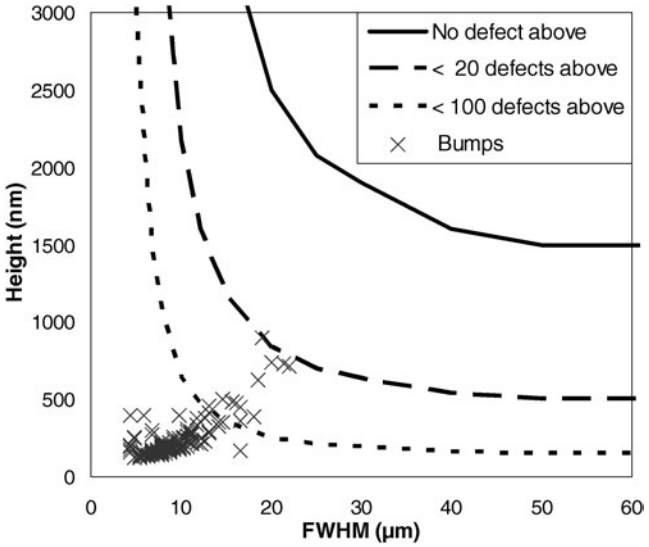

Fig. 11. Bumps characterized with DHM on >50% of microshell surface.

of this microshell is declared to be acceptable, according to other specifications, in particular, the one about roughness for higher deformation modes.

Also, specification curves permit validation of the threshold level applied in preprocessing of DHM images. In fact, all bumps with a height <120 nm are not above the dotted curve until an FWHM of 60 μm and so no restriction is asked in their number.

We have first characterized a microshell on regions corresponding to five equator scans. In this configuration, more than half of the entire outer surface is covered and gives a statistical counting of the bumps (see Fig. 11). Each band or equator is composed of 72 images.

Results of this "half"-characterization with DHM are

1. 160 bumps counted
2. 0 bumps above the line curve (tolerance = 0 for complete surface)
3. 1 bump above the dashed curve (tolerance = 20 for complete surface)
4. 12 bumps above the dotted curve (tolerance = 100 for complete surface)
5. mean height = 230 nm
6. mean FWHM = 9 μm.

The same microshell has been characterized with a full sphere mapper technique. The entire surface is scanned with five bands covering. Each band corresponds to 16 parallel profiles. Figure 12 presents a raw scanned band on the microshell previously analyzed by DHM. On each profile, peaks are associated with bump presence and peak parameters are considered to be bump parameters

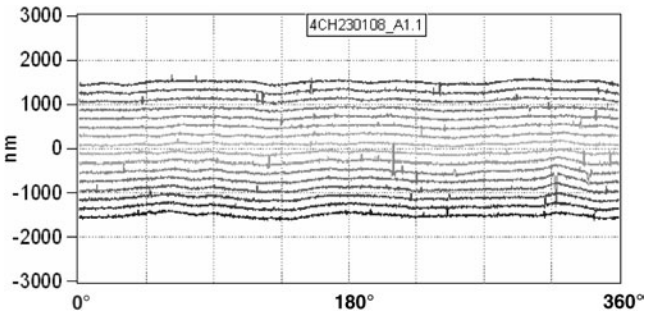

Fig. 12. Characterization of a microshell along a band with sphere mapper.

(height and width). Very large bumps (>40 μm FWHM) are observed on adjacent profiles. These profiles also allow one to study the deformation modes of the microshell. The analysis of roughness enables one to plot a power spectrum corresponding to microshell deformation and to obtain RMS values for different mode scales.

Table I presents the values of modes determined from the mean power spectrum that characterizes the entire outer surface of the microshell.

In a second part, the analysis of the peaks on the five bands permits listing of all the bumps accessible on the outer surface of the microshell. We can also represent them on specification curves as shown in Fig. 13.

A similar threshold level at 120 nm is applied to the data in order to compare the same bump counting with DHM.

The results of the characterization with the sphere mapper are

TABLE I

Roughness Determined with a "Full" Sphere Mapper Technique

	Deformation Modes						
	2	3–10	11–50	51–100	12–120	101–1000	>10
RMS (nm)	19	29	10	6	11	9	14

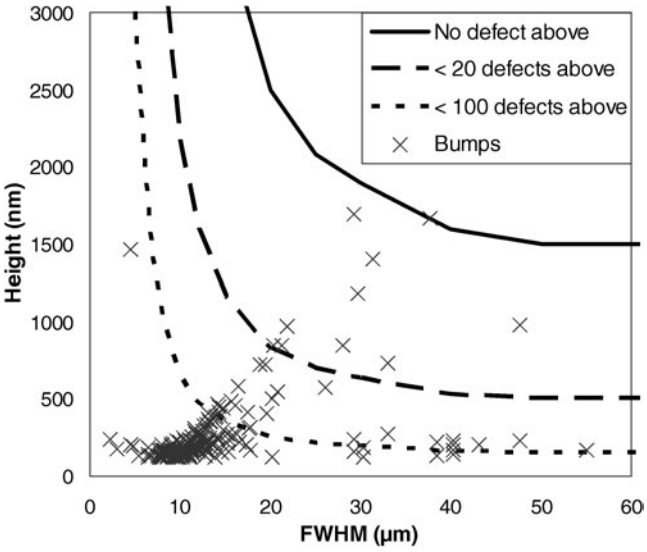

Fig. 13. Bumps characterized with sphere mapper of the entire microshell surface.

1. 209 bumps counted
2. 0 bumps above the line curve (tolerance = 0 for complete surface)
3. 10 bumps above the dashed curve (tolerance = 20 for complete surface)
4. 42 bumps above the dotted curve (tolerance = 100 for complete surface)
5. mean height = 265 nm
6. mean FWHM = 15 μm.

The number of bumps counted with the sphere mapper is, relative to the scanned surface ratio, lower than the one counted with DHM. In fact, all the bumps that can be present between two adjacent profiles (with a width <40 μm) will not be counted with AFM techniques. This consideration together with the lateral resolution of 2 μm (3600 points along an equator) explains also that the mean FWHM of bumps is higher with the sphere mapper than with DHM. The mean height of bumps is comparatively the same with both techniques.

Finally, DHM characterization of the outer surface of a microshell is more accurate than the one with the sphere mapper, because the entire surface is really scanned with a 400-nm lateral resolution. Moreover, the acquisition time needed by DHM is much shorter to explore the entire surface of the microshell.

V. CONCLUSION

To characterize the outer surface of a microshell produced for ignition applications, DHM is proved to be very well adapted with respect to subnanometric axial resolution and high acquisition rates. Local defects on the surface (bumps) are easily displayed, and data processing allows one to make an efficient counting of them. Each bump is defined with its localization, height, and FWHM. These parameters are used in reference with specification curves, which define the isolated feature specifications, and validate the quality of the microshell.

REFERENCES

1. J. D. LINDL, *Inertial Confinement Fusion*, Springer-Verlag, New York (1998).

2. M. THEOBALD, P. BACLET, O. LEGAIE, and J. DURAND, "Properties of a-C:H Coatings Prepared by PECVD for Laser Fusion Targets," *Fusion Technol.*, **38**, 62 (2000).

3. B. DUMAY et al., "Atomic Force Microscopy Investigation of a-C:H Films Prepared by PECVD for Inertial Confinement Fusion Experiments," *J. Vac. Sci. Technol.*, **20**, 366 (2002).

4. M. THEOBALD, C. CHICANNE, J. BARNOUIN, E. PECHE, and P. BACLET, "Gas Etching to Obtain Germanium Doped CH_x Microshells Compatible with the Laser Megajoule Target Specifications," *Fusion Sci. Technol.*, **49**, 757 (2006).

5. S. W. HAAN et al., "Update on Ignition Target Fabrication Specifications," *Fusion Sci. Technol.*, **41**, 164 (2002).

6. M. THEOBALD, O. LEGAIE, P. BACLET, and A. NIKROO, "Thick GDP Microshells for LIL and LMJ Targets," *Fusion Sci. Technol.*, **41**, 238 (2002).

7. R. B. STEPHENS, D. OLSON, H. HUANG, and J. B. GIBSON, "Complete Surface Mapping of ICF Shells," *Fusion Sci. Technol.*, **45**, 210 (2004).

8. D. GABOR, "A New Microscopic Principle," *Nature*, **161**, 777 (1948).

9. U. SCHNARS and W. P. O. JUPTNER, "Digital Recording and Numerical Reconstruction of Holograms," *Meas. Sci. Technol.*, **13**, R85 (2002).

10. T. C. POON, *Digital Holography and Three-Dimensional Display*, Springer, New York (2006).

11. Lyncée Tec, available on the Internet at www.lynceetec.com.